


Jian Ni

# A Simulation of Biomes on the Tibetan Plateau and Their Responses to Global Climate Change



*The improved process-based equilibrium terrestrial biosphere model (BIOME3China) was run under the present climate to model the potential biomes on the Tibetan Plateau on a 10' grid. The simulated biome was basically in good*

*agreement with a potential natural vegetation map based on a numerical comparison between two maps using the  $\Delta V$  statistic ( $\Delta V = 0.38$ ). A coupled ocean-atmosphere general circulation model including sulfate aerosols was used to drive a double greenhouse gas scenario to the end of the next century. The simulated vegetation under changed climate with a  $CO_2$  concentration of 500 ppmv and a baseline biome map were also compared using the  $\Delta V$  statistic ( $\Delta V = 0.4$ ). The climate change would cause a large reduction in the temperate desert, alpine steppe, desert, and ice/polar desert, a large increase in the cold-temperate conifer forest, temperate shrubland/meadow, and temperate steppe, and a general northwestward shift of all vegetation zones. In addition to simulation of biome distribution, BIOME3China also predicted net primary production (NPP) of each grid cell. Comparisons between predicted annual NPP and 160 forest NPP measurements show an agreement between them with a linear regression, despite many problems, such as the quality of the field data. The pattern of predicted annual NPP in the scenario with enhanced  $CO_2$  concentration was the same as that under the present climate; however, the NPP of each biome would increase significantly. Present permafrost simulated using the air frost index was quite similar to the actual frozen ground distribution on the Tibetan Plateau. After the change in climate, the boundary between continuous and discontinuous permafrost would shift toward the north of the plateau by about  $1\text{--}2^\circ$  in latitude. The continuous permafrost would mostly disappear, whereas the no-permafrost area would greatly increase. The movement of permafrost would take place with the shift of vegetation zones to the north. The disappearance of permafrost and the expansion of no-permafrost areas would accelerate the desertification of the Tibetan Plateau.*

**Keywords:** biome simulation; response to global climate change; Tibetan Plateau; terrestrial system modeling.

**Peer reviewed:** September 1999. **Accepted:** October 1999.

## Introduction

The Tibetan Plateau, with an average altitude of about 5000 m, is one of the most important regions in the world. It affects terrestrial ecosystems in China because of its unique location, high elevation (topography), and special climate systems (Zhang 1983). The biomes on the Tibetan Plateau are special (Zhang 1983). The reason is that the plateau biomes are not completely tundra and ice, as simulated by some global models, eg, TEM (Melillo et al 1993; Xiao et al 1998), BIOME1 (Prentice et al 1992), and BIOME3 (Haxeltine and Prentice 1996). In fact, there is special high-cold vegetation at three altitudinal levels, ie, subnival and nival (ca >5200 m above sea level [asl]); alpine meadow and scrubland, alpine steppe and shrubland, alpine desert in the central plateau, plateau temperate steppe, and plateau temperate desert in the periphery (ca 4000–5200 m asl); and tropical and subtropical mountain forests in the southern Himalayan mountains and sub-alpine conifer forests in the southeastern part of the plateau (ca <4000 m asl) (Editorial Committee for Vegetation of China 1980; Zhang et al 1996). The vertical and horizontal vegetation distribution on the Tibetan Plateau was simulated with climatic warming (Zhang et al 1996). Horizontal vegetation distribution is very sensitive and vulnerable to global change, mainly because the Tibetan Plateau is located in marginal land areas where the growth and distribution of plants depend heavily on local climate conditions (Zhang et al 1996). It can therefore be used as an indicator for monitoring global climate change (Zhang et al 1996).

The biomes of the world, including the Tibetan Plateau, were simulated by different global models, eg, the biogeography model (BIOME1: Prentice et al 1992), the biogeochemistry model (TEM: Melillo et al 1993; McGuire et al 1997), a combination of these two types (BIOME3: Haxeltine and Prentice 1996), and the integrated biosphere model of land surface processes, terrestrial carbon balance, and vegetation dynamics (IBIS: Foley et al 1996). Chinese biomes were recently also predicted by BIOME3 (Ni et al 1999) and TEM (Xiao et al 1998). In these simulations, the biome types of the Tibetan Plateau were mainly considered as tundra and ice/polar desert owing to prediction at global and regional scales. Nevertheless, special high-cold vegetation, as described above, does exist. Therefore, the simulation of biomes and their response to global change on the Tibetan Plateau should be improved at a local scale to avoid confusion and mistakes due to very simple biome classification.

Zhang et al (1996) studied the response of natural vegetation on the Tibetan Plateau to global climate change using several bioclimatic methods, such as the Holdridge life zone classification system, the montane

vegetation belt system, the permafrost model, and the improved net primary production (NPP) model. However, Zhang et al (1996) used statistical models. The simulation of biomes was not numerically compared with the potential natural vegetation distribution. Modeled NPP was not compared with observed NPP. The scenarios used in the paper were for increments of 4°C temperature and 10% precipitation, but did not involve output of general circulation models (GCMs). The CO<sub>2</sub> ecophysiological effect was not taken into account.

Zheng (1996) classified the physico-geographical regions system of the Tibetan Plateau based on thermal conditions (days of above 10°C daily mean temperature and mean temperature of the warmest month), moisture regimes (annual aridity index, ie, evapotranspiration/precipitation and annual precipitation), and variation in landform (topography). This is a new physico-geographical regions system, but the ecophysiological constraints of plants, as shown in the papers of Prentice et al (1992) and Haxeltine and Prentice (1996), were not yet considered.

In this study, a simulation of biomes on the Tibetan Plateau was made using BIOME3China, an improved version of the equilibrium biosphere-atmosphere model BIOME3 (Haxeltine and Prentice 1996). The responses of biomes to changed climate and elevated CO<sub>2</sub> under a GCM scenario at the Hadley Centre (Johns et al 1997; Mitchell et al 1995) are also modeled. At the same time, BIOME3China simulates the annual NPP of each biome at the present climate and scenario. Permafrost at the present climate and its response to climate warming are predicted, with the simulation of vegetation and NPP on the Tibetan Plateau at a local scale.

## Methods

### The BIOME3China model

The equilibrium terrestrial biosphere model, BIOME3 (Haxeltine and Prentice 1996), combining the biogeography and biogeochemistry modeling approaches in a single global framework, simulates vegetation distribution and biogeochemistry and couples vegetation distribution directly to biogeochemistry.

The improved BIOME3 for Chinese vegetation (BIOME3China) followed most of the algorithms and rules of BIOME3. Model inputs were atmospheric CO<sub>2</sub> concentration, latitude, soil texture, absolute minimum temperature, and monthly climate (temperature, precipitation, and cloudiness) data. Model output consisted of a quantitative description of the state of vegetation in terms of the dominant plant functional type (PFT), secondary PFTs present, the total leaf area index (LAI), and NPP for the ecosystem. In addition to information on the dominant PFT, other potentially present PFTs, and the total LAI, the classification scheme used

the following subsidiary variables: annual average available soil moisture expressed as a percentage, monthly average available soil moisture, temperature of the coldest month ( $T_{cm}$ ), and growing degree-days on a 5°C base ( $GDD_5$ ) and on a 0°C base ( $GDD_0$ ). Following BIOME3, BIOME3China used nine PFTs, which were tropical broad-leaved evergreen, tropical broad-leaved raingreen, temperate broad-leaved evergreen, boreal/temperate summergreen, and boreal/temperate evergreen conifer, cool grass and warm grass. Eleven biomes (Table 1) were used for the simulation and prediction of vegetation on the Tibetan Plateau.

The Tibetan Plateau has a very high elevation, resulting in very low temperatures. Under extreme climatic conditions, BIOME3 has a problem mapping biomes. The problem arose because the function used to inhibit photosynthesis at low temperatures is a generic function (Haxeltine and Prentice 1996), whereas in reality, plants in cold environments have mechanisms that allow them to photosynthesize at lower temperatures than other plants. BIOME3 therefore seems to underestimate photosynthesis in alpine plants, and NPP was then predicted to be very low or even zero. Moreover, the modeled vegetation distribution of BIOME3 is partially determined by modeled NPP, while vegetation type in turn affects NPP (Haxeltine and Prentice 1996). Using this novel design, the model cannot successfully produce the patterns in potential natural vegetation for the current climate. The ecophysiological constraints of plants in alpine tundra ( $GDD_5 < 350$ ) and ice/polar desert ( $GDD_0 < 150$ ) modeled by BIOME3 on the central Tibetan Plateau, therefore, should be completely modified. Zheng (1996) provided good thermal and moisture regimes for the Tibetan Plateau. The classification scheme of arctic/alpine tundra and ice/polar desert used to map model output to biomes is shown in Table 1, based on Zheng (1996). Only  $GDD_0$  and annual precipitation were used for the high-cold vegetation (Table 1). Other schemes followed BIOME3 (table 5 in Haxeltine and Prentice 1996).

### Climate data

Data on monthly mean temperature, absolute minimum temperature, precipitation, and percent of sunshine hours for 841 standard weather stations between 1951 and 1980 in China (Chinese Central Meteorological Office 1984) were interpolated using the smoothing spline method (Hutchinson 1989). The data for Tibet were extracted between 73 and 105°E and 27 and 40°N on 10' grid cells.

### Soil data

A soil-texture data set for the Tibetan Plateau was constructed on 10' grid cells based on the textural information digitized from Xiong and Li (1987). Seven categories, ie, coarse, medium, fine, medium-coarse, fine-

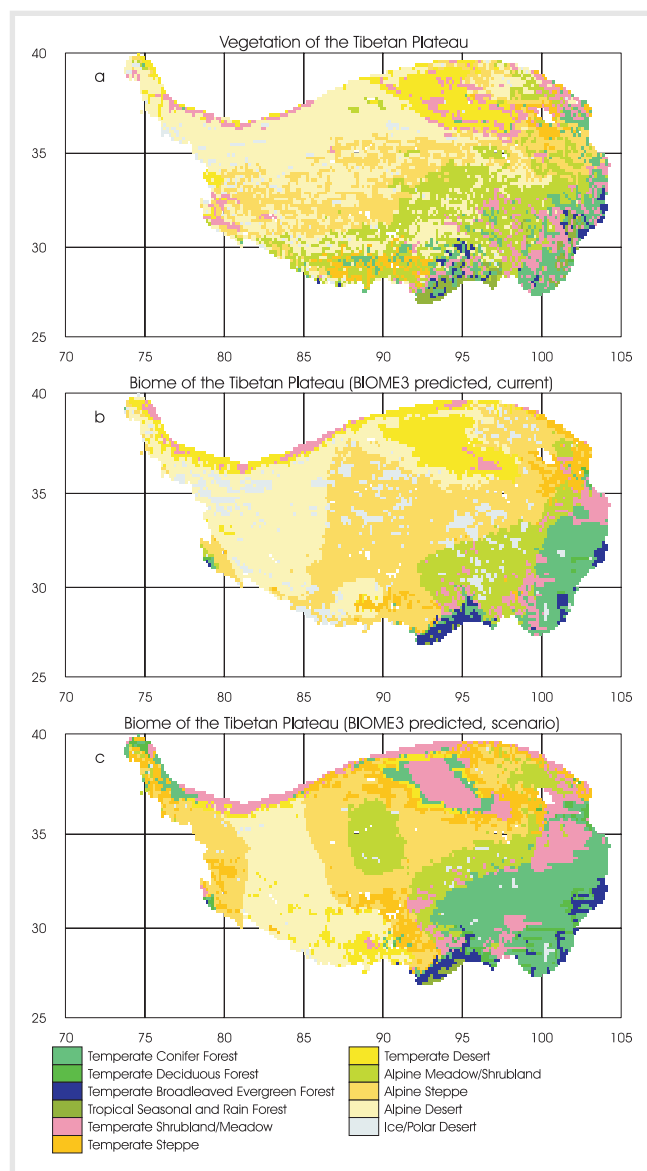


**FIGURE 1** Biomes on the Tibetan Plateau. **a.** Potential natural vegetation based on Vegetation Map of China (Hou et al 1982). **b.** Biomes predicted by BIOME3China under the present climate with a CO<sub>2</sub> concentration of 340 ppmv. **c.** Biomes predicted by BIOME3China under a future climate scenario at the Hadley Centre GCM (Johns et al 1997; Mitchell et al 1995) with a CO<sub>2</sub> concentration of 500 ppmv.

coarse, fine-medium-coarse, and medium-fine, were assigned for use in the present study.

#### Vegetation data

A map of potential natural vegetation of the Tibetan Plateau (Figure 1a) on 10' grid cells was constructed from a digital vegetation map, which consists of 113 vegetation units digitized from the "Vegetation Map of

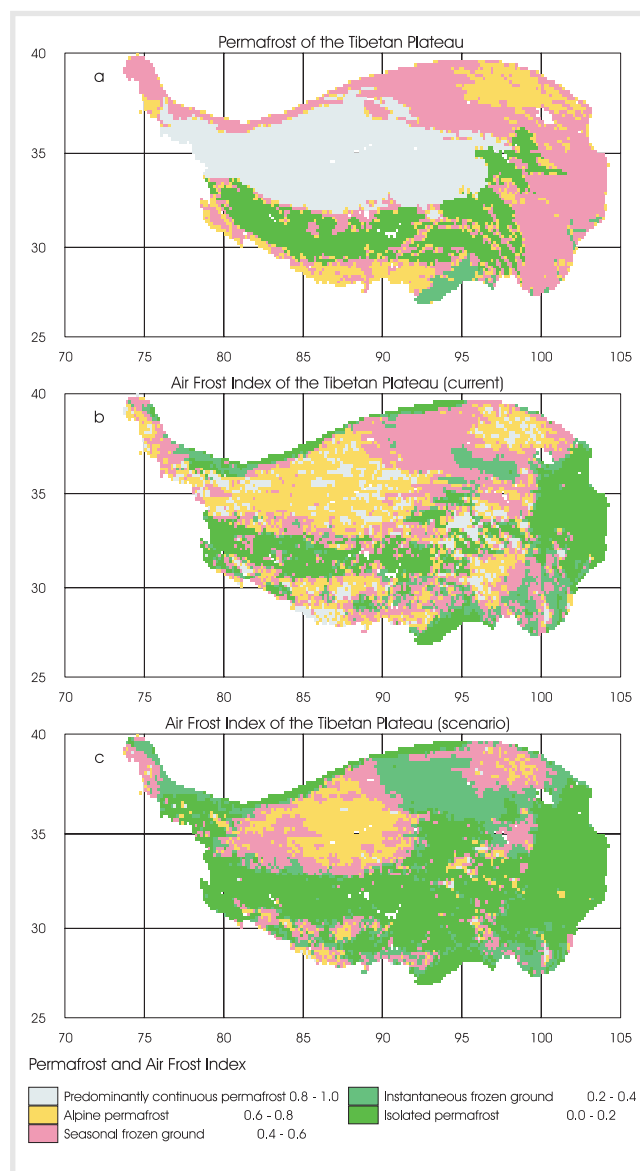


**FIGURE 2** Permafrost on the Tibetan Plateau. **a.** Natural permafrost based on observation. **b.** Permafrost predicted by air frost index (Nelson and Outcalt 1987) at present climate with a CO<sub>2</sub> concentration of 340 ppmv. **c.** Permafrost predicted by air frost index (Nelson and Outcalt 1987) under a future climate scenario at the Hadley Centre GCM (Johns et al 1997; Mitchell et al 1995) with a CO<sub>2</sub> concentration of 500 ppmv.

China" at a scale of 1:4,000,000 (Hou et al 1982). These units were assigned to 11 categories (Table 1) for use in the BIOME3China model.

#### Permafrost

Figure 2a shows a geographical distribution of frozen ground on 10' grid cells, digitized on the basis of data observed on the Tibetan Plateau. An air frost index

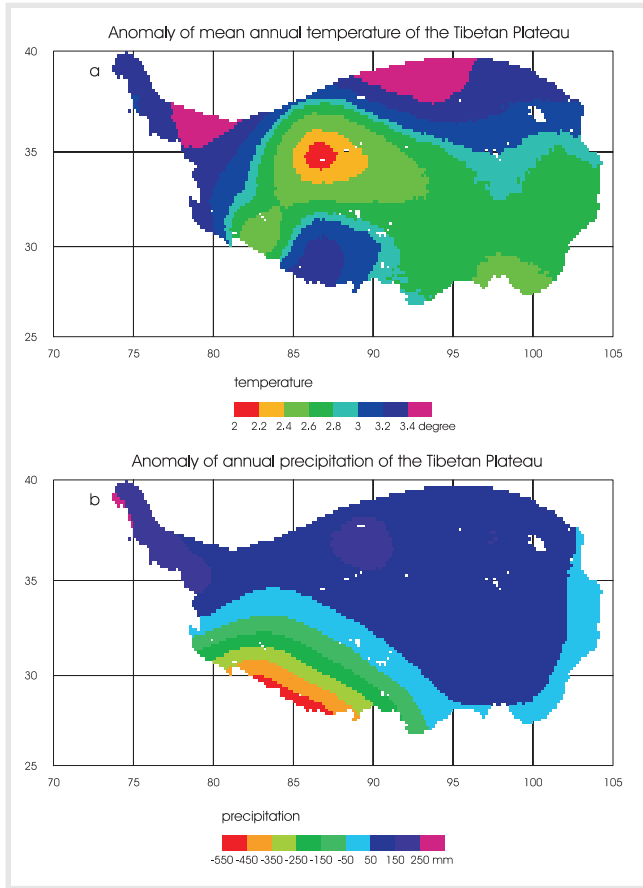


**FIGURE 3** Anomalies in (a) annual mean temperature and (b) annual precipitation on the Tibetan Plateau simulated by the Hadley Centre GCM (Johns et al 1997; Mitchell et al 1995).

(*AFI*) according to Nelson and Outcalt (1987) is often used to quantify the geographical distribution of permafrost, and is expressed as

$$AFI = DDF^{1/2} / (DDF^{1/2} + DDT^{1/2}).$$

*DDF* and *DDT* are the freezing and thawing indices (°C day) for a study area, respectively. The two indices can be calculated from  $DDF = -T_w L_w$  and  $DDT = T_s L_s$ , where

$$\begin{aligned} T_w &= T - A(\sin A / (3.14 - B)), \\ T_s &= T + A((\sin B) / B), \\ L_w &= 365 - L_s, \\ L_s &= 365(B / 3.14), \end{aligned}$$

and

$$\begin{aligned} T &= (T_{\max} + T_{\min}) / 2, \\ A &= (T_{\max} - T_{\min}) / 2, \\ B &= \cos^{-1}(-T/A), \end{aligned}$$

where  $T_{\max}$  and  $T_{\min}$  are, respectively, the air temperatures of the warmest and coldest months. Therefore,  $T$  and  $A$  approximately define the annual mean air temperature and the amplitude of annual temperature cycle, respectively.  $B$  is the frost angle defined as a point along the time axis at which the annual temperature curve crosses the line 0°C.

No permafrost can be observed in areas with an *AFI* less than 0.4, while permafrost is continuously distributed in areas where the *AFI* is above 0.6. In areas with an *AFI* between 0.4 and 0.6, the distribution of permafrost is intermittent rather than continuous.

### Scenario

Climate output from the Hadley Centre ocean-atmosphere GCM (Johns et al 1997; Mitchell et al 1995), including the effects of both greenhouse gases (GHGs) and sulfate aerosols, was used. The scenario was driven by computing the averages for 1931–1960 and for 2070–2099 from the climate model simulation and then interpolating the anomalies to the grid in high resolution (Figure 3a,b). These were then added to the baseline climate to produce the climate fields used to drive BIOME3China. The emissions scenario (IPCC WGI 1996) included an increase in atmospheric CO<sub>2</sub> concentration from 340 to 500 ppmv in the doubled GHGs simulation. Simulations were performed with the BIOME3China model for the present climate and a CO<sub>2</sub> concentration of 340 ppmv and for the doubled GHGs climate with physiological CO<sub>2</sub> effects calculated using an atmospheric CO<sub>2</sub> concentration of 500 ppmv. Thus, the equilibrium response of vegetation to the changed climate and CO<sub>2</sub> was simulated.

### Results

#### Biome distribution

The model produced a total of 11 unique biomes (Figure 1b). Visual comparison of predicted biome distributions with their natural equivalents indicated good agreement. This impression was supported by the overall value 0.38 of the  $\Delta V$  statistic (Sykes et al 1999) for the two maps.

$\Delta V$  is a nontrivial and attribute-based measure of dissimilarity between biomes (Sykes et al 1999). Dissimilarity between two maps ( $\Delta V$ ) was obtained by area-weighted averaging of  $\Delta V$  over the model grid, suggesting that  $\Delta V$  values <0.15 can be considered excellent, values of 0.15–0.3 very good, values of 0.3–0.45 good, values of 0.45–0.6 fair, values of 0.6–0.8 poor, and values >0.8 very poor.

The  $\Delta V$  values (area-weighted averages across grid cells) of each biome for comparisons between baseline simulations with BIOME3China and natural potential vegetation are shown in Table 2. The values show excel-

| Biome   | GDD <sub>0</sub> (°C) | Precipitation (mm) |
|---|-----------------------|--------------------|
| Cold-temperate conifer forest <sup>a</sup>                |                       |                    |
| Temperate deciduous broad-leaved forest <sup>b</sup>      |                       |                    |
| Warm-temperate evergreen broad-leaved forest <sup>b</sup> |                       |                    |
| Tropical seasonal and rain forest <sup>c</sup>            |                       |                    |
| Temperate shrubland/scrub <sup>d</sup>                    | 1200–2500             | 500–650            |
| Temperate steppe <sup>e</sup>                             | 1200–2500             | 250–500            |
| Temperate desert  | 1200–2500             | <250               |
| Alpine meadow   | 100–1200              | 500–650            |
| Alpine steppe   | 100–1200              | 250–500            |
| Alpine desert   | 100–1200              | <250               |
| Ice/Polar desert  | <100                  |                    |

<sup>a</sup>The biome combined boreal deciduous conifer, boreal evergreen conifer, temperate/boreal mixed and temperate conifer forests in BIOME3 (Haxeltine and Prentice, 1996). The ecophysiological constraints correlate with BIOME3.

<sup>b</sup>The biomes and their constraints are the same as those in BIOME3.

<sup>c</sup>The biome combined tropical seasonal forest and rain forest in BIOME3. Their constraints correlate with BIOME3.

<sup>d</sup>The biome combined arid shrubland and scrub in BIOME3. Other constraints, except for those listed in the table, correlate with BIOME3.

<sup>e</sup>The biome combined moist savannas, dry savannas, temperate tall grassland and short grassland in BIOME3. Constraints correlated with BIOME3 except for those listed in the table.

**TABLE 1** Biomes on the Tibetan Plateau used in BIOME3China and their climatic constraints. All constraints of each biome correlate with BIOME3 except for those listed in the table.

lent agreement for temperate desert; very good agreement for temperate steppe; good agreement for temperate deciduous broad-leaved forest, alpine meadow/shrubland, alpine steppe, and alpine desert; fair agreement for cold-temperate conifer forest, warm-temperate evergreen broad-leaved forest, tropical seasonal and rain forest, and ice/polar desert; and poor agreement for temperate shrubland/meadow.

The simulated vegetation under changed climate with a CO<sub>2</sub> concentration of 500 ppmv (Figure 1c) and a baseline biome map (Figure 1b) were also compared using the  $\Delta V$  statistic (Sykes et al 1999). The total  $\Delta V$  value was 0.4. The larger dissimilarities occurred in temperate shrubland/meadow, temperate steppe, temperate desert, alpine meadow/shrubland, and ice/polar desert between present and changed climate. The climate change, with the inclusion of physiological CO<sub>2</sub> effects, produced a large reduction in the temperate desert, alpine steppe, desert and ice/polar desert; a large increase in the cold-temperate conifer forest, temperate shrubland/meadow, and temperate steppe (Table 2); and a general northwestward shift of all belts (Figure 1).

### Permafrost distributions

Permafrost is a very important climatic factor on the Tibetan Plateau and a sensitive indicator of climate change. A geographic distribution of frozen ground (Figure 2b) on the Tibetan Plateau at present, which is

simulated using *AFI* (Nelson and Outcalt 1987), was quite similar to the actual frozen ground distribution (Figure 2a). For changed climate in the future, permafrost—especially areas of predominantly continuous permafrost, alpine permafrost, and seasonal frozen ground (*AFI* > 0.4)—would decrease on the Tibetan Plateau (Figure 2b,c). Areas of nonpermafrost (*AFI* < 0.4), however, would largely increase (Figure 2b,c).

### Discussion

The Tibetan Plateau is one of the Earth's unique physico-geographical regions. Generally, the spatial differentiation of physico-geographical regions on the plateau is determined mainly by topographic configuration and atmospheric circulation, warm and humid in the southeast and cold and arid in the northwest (Zheng 1996). In these districts, temperature and precipitation decrease gradually with the increment in latitude, indicating that the climatic resources controlling plant growth diminish from the southeastern regions to the northwestern regions. The reduction in climatic resources toward the northwest is the most important reason for the simplification of species complexity in vegetation and of regional differentiation in vertical vegetation (Zhang et al 1996). The vegetation type in this district changes gradually from marine humid montane (tropical seasonal and rain forest, warm-temperate broad-leaved evergreen forest, temperate deciduous

**TABLE 2** Changes of area ( $\times 1000 \text{ km}^2$ ) and  $\Delta V$  values for each biome of the Tibetan Plateau. A, areas of potential biome predicted by the BIOME3China model under current climate with  $\text{CO}_2$  concentration 340 ppmv; B, areas of biome predicted by the BIOME3China model based on a scenario at the end of the next century with an enhanced  $\text{CO}_2$  concentration of 500 ppmv; C,  $\Delta V$  values for comparison between potential biome predicted by BIOME3China at the current climate and actual vegetation distribution; D,  $\Delta V$  values for comparison between future biome distribution under a scenario with a  $\text{CO}_2$  concentration of 500 ppmv and potential biome under the current climate with a  $\text{CO}_2$  concentration of 340 ppmv predicted by BIOME3China.

| Biome  | Areas ( $\times 1000 \text{ km}^2$ ) |                | $\Delta V$  |             |
|--|--------------------------------------|----------------|-------------|-------------|
|  | A                                    | B              | C           | D           |
| Cold-temperate conifer forest                | 183.61                               | 448.61         | 0.55        | 0.14        |
| Temperate deciduous broad-leaved forest      | 7.50                                 | 49.44          | 0.37        | 0.17        |
| Warm-temperate evergreen broad-leaved forest | 45.28                                | 60.56          | 0.45        | 0.18        |
| Tropical seasonal and rain forest            | 2.50                                 | 9.17           | 0.56        | 0.33        |
| Temperate shrubland/meadow                   | 139.17                               | 315.83         | 0.63        | 0.59        |
| Temperate steppe                             | 83.06                                | 254.17         | 0.26        | 0.54        |
| Temperate desert                             | 246.94                               | 104.72         | 0.12        | 0.57        |
| Alpine meadow/shrubland                      | 252.50                               | 299.44         | 0.37        | 0.81        |
| Alpine steppe                                | 755.00                               | 547.78         | 0.31        | 0.21        |
| Alpine desert                                | 597.22                               | 411.39         | 0.35        | 0.34        |
| Ice/polar desert                             | 210.28                               | 21.94          | 0.52        | 0.72        |
| <b>Total</b>                                 | <b>2523.10</b>                       | <b>2523.10</b> | <b>0.38</b> | <b>0.40</b> |

forest, and conifer forest) in the southeastern region to continental semiarid montane (temperate shrubland/meadow, steppe, alpine meadow/shrubland, and steppe) in the middle region to continental arid montane (temperate desert, alpine desert, and ice/polar desert) in the northwestern region (Figure 1a). BIOME3China simulated the biome distribution with generally good agreement in central and northwestern Tibet ( $\Delta V = 0.36$  for nonforests) based only on climatic constraints (GDD0 and precipitation) and with fair agreement in the southeast ( $\Delta V = 0.48$  for forests) based on both climatic conditions and biogeochemical factors (Table 2). This vegetation pattern is similar to that modeled by Zhang et al (1996) using the Holdridge life zone classification system. The problem is that the actual vegetation distribution in Tibet is mosaic (Figure 1a), but the biome predicted by BIOME3China was mostly continuous (Figure 1b). The predicted alpine steppe biome moved further north (Figure 1b) than its actual distribution (Figure 1a). Four forest types and alpine meadow/shrubland modeled by BIOME3China were concentrated only in the southeastern region (Figure 1b), but their actual distribution could expand to the southern and central Plateau (Figure 1a). The reason is that the actual vegetation was derived from the digitized vegetation map of China. The actual distribution of vegetation on the Tibetan Plateau was determined not only by climate but also by soil, topography, and human disturbance, which is usually extreme in terms of spatial heterogeneity. On the other hand, potential vegetation driven by the interpolated continuous climatic data and by constraints in a

large range would be mostly continuous when climate conditions are similar around one place.

The great expansion in human activity is causing significant changes in natural conditions. Among these changes, the increase in GHGs is expected to have great impact on climate and very important implications for the broad-scale distribution of terrestrial ecosystems (IPCC WGI 1996), especially in the mountains (Haslett 1997). A recent study by a Chinese scientist (Liu et al 1998) shows that the Plateau climate has generally been warming during this century and precipitation has generally been increasing over the last 30 years. According to climate output from the Hadley Centre GCM (Johns et al 1997; Mitchell et al 1995), temperature will increase  $2\text{--}3.6^\circ\text{C}$  by the end of the next century in the Plateau, and precipitation will increase by  $0\text{--}300 \text{ mm}$  in the central and eastern parts of the Plateau and decrease by  $0\text{--}550 \text{ mm}$  in the southwest (Figure 3a,b). The greatest increases in temperature, by  $3.0\text{--}3.6^\circ\text{C}$ , are expected to occur in the north and the southwest. An increase of  $2.0\text{--}3.0^\circ\text{C}$  will occur in the central and eastern Plateau (Figure 3a). The greatest increases are likely to be in the winter. The pattern of precipitation on the Tibetan Plateau might change gradually, from an increase in the north to a decrease in the southwest (Figure 3b). After climate change with  $\text{CO}_2$  concentration of 500 ppmv, biomes of the Plateau shifted significantly to the north and northwest (Figure 1c). The  $\Delta V$  value of each biome between the current climate and the scenario reflected the dissimilarity of the biome under different climatic conditions. The greater the  $\Delta V$  value, the greater the dissimilarity of biome between present climatic conditions



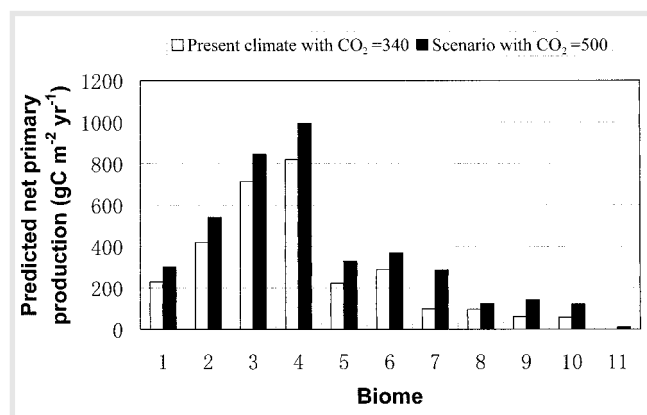


**FIGURE 4** BIOME3China-predicted annual NPP for each biome on the Tibetan Plateau and their responses to climate change with enhanced  $\text{CO}_2$  concentration. 1, cold-temperate conifer forest; 2, temperate deciduous broad-leaved forest; 3, warm-temperate evergreen broad-leaved forest; 4, tropical seasonal and rain forest; 5, temperate shrubland/meadow; 6, temperate steppe; 7, temperate desert; 8, alpine meadow/shrubland; 9, alpine steppe; 10, alpine desert; 11, ice/polar desert.

and the scenario (Sykes et al 1999). In addition to a great reduction in the area of temperate desert, alpine steppe, desert, and ice/polar desert and a large increase in the area of cold-temperate conifer forest, temperate shrubland/meadow, and temperate steppe, great change would occur in temperate shrubland/meadow, temperate steppe, temperate desert, alpine meadow/shrubland, and ice/polar desert under changed climatic conditions (Table 2). Meadow, shrubland, and steppe would increase in area because increased temperature and water stress favor  $\text{C}_4$  grasses over  $\text{C}_3$  woody plants. With the inclusion of physiological  $\text{CO}_2$  effects, however, there would be a marked decrease in the area occupied by temperate desert, alpine desert, and ice/polar desert (Table 2). This may be due to  $\text{C}_3$  plants becoming more competitive relative to  $\text{C}_4$  grasses as well as a general reduction in stomatal conductance, which favors the dominance of woody plants by reducing water stress.

The response of life zones on the Tibetan Plateau to climate change predicted by Zhang et al (1996) showed that natural vegetation would shift northward from each present position due to climate warming. This changing pattern is quite similar to that described in the present paper. Tropical and subtropical forests and montane and alpine steppe will increase in area. Ice and polar (frigid) desert will decrease in area. These predictions are similar to those of Zhang et al (1996). The difference is that conifer forest and alpine meadow would largely decrease, while montane and alpine deserts would significantly increase according to Zhang, whereas the opposite is true in the present study. This may be because Zhang et al (1996) considered only an increase in temperature and precipitation of 4° and 10%, respec-

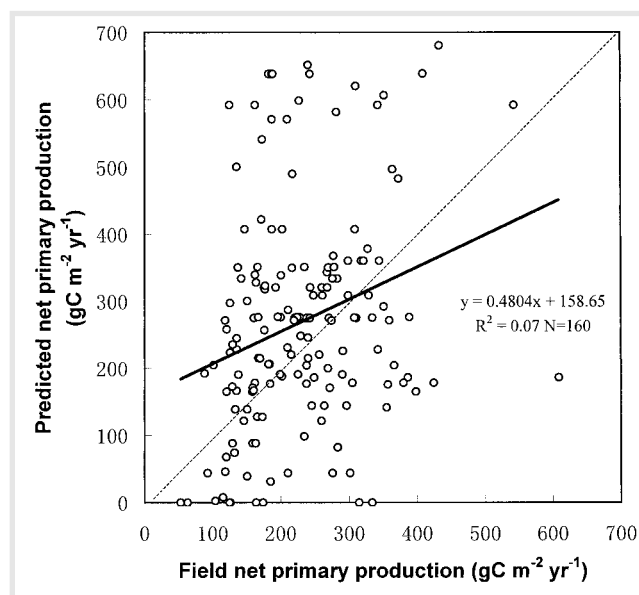


**FIGURE 5** Comparison between NPP field measurements and BIOME3China-predicted annual NPP. The field NPP data are derived from the Chinese Forest NPP database (Ni and Zhang unpublished manuscript). NPP measurements are compared to the predicted NPP for the 10' grid square within which each measurement site is located. The solid line shows a linear regression of predicted NPP against measurements, and the broken line indicates exact agreement.

tively. In the present study, however, both GCM output and  $\text{CO}_2$  concentration were taken into account. On the other hand, the difference between biome classification in this paper and the Holdridge life zone in Zhang et al (1996) might result in dissimilarities.

Continuous global climate change is expected to have an impact not only on biome geographic distributions but also on biogeochemical cycles in the terrestrial ecosystem. In addition to simulation of biome distribution, BIOME3China also predicted NPP for each grid cell. Under present climatic conditions, tropical, warm-temperate, and temperate forests would have the highest annual NPP (ca 220–810  $\text{gC}/\text{m}^2/\text{y}$ ). Temperate meadow/shrubland, steppe, and desert would have an intermediate NPP (250–290  $\text{gC}/\text{m}^2/\text{y}$ ). The lowest production was found in alpine meadow/shrubland, steppe, and desert, whereas predicted annual NPP for ice/polar desert was zero (Figure 4). Although there was a lack of NPP data for meadow, steppe, and desert on the Plateau, 160 forest NPP data were obtained from the Chinese Forest NPP database (Ni and Zhang unpublished manuscript). A comparison was made between predicted annual NPP and 160 field forest NPP measurements (Figure 5). There are many problems associated with such comparisons, including the quality of the data and the fact that the model simulated the average NPP over a grid square, while NPP measurements were

made at particular sites (Haxeltine and Prentice 1996). Some sites with positively measured NPP had zero predicted NPP on the Tibetan Plateau (Figure 5) owing to very high elevation with very low temperatures. Despite these problems, the resulting comparison showed an agreement between the predicted NPP and measurements with a linear regression (Figure 5).

If climate change and CO<sub>2</sub> concentration enrichment occur at the end of the next century, production in terrestrial ecosystems will be changed corresponding-

ly. The pattern of predicted annual NPP in the scenario with a CO<sub>2</sub> concentration of 500 ppmv was the same as that for the present climate, but the NPP of all biomes increased significantly (Figure 4). This may be largely because of the positive effects of increased CO<sub>2</sub>, precipitation, and temperature in most of regions on the Tibetan Plateau.

The frozen ground is formed and maintained by severe climate in winter. It is very sensitive to temperature change. Therefore, the area of frozen ground,

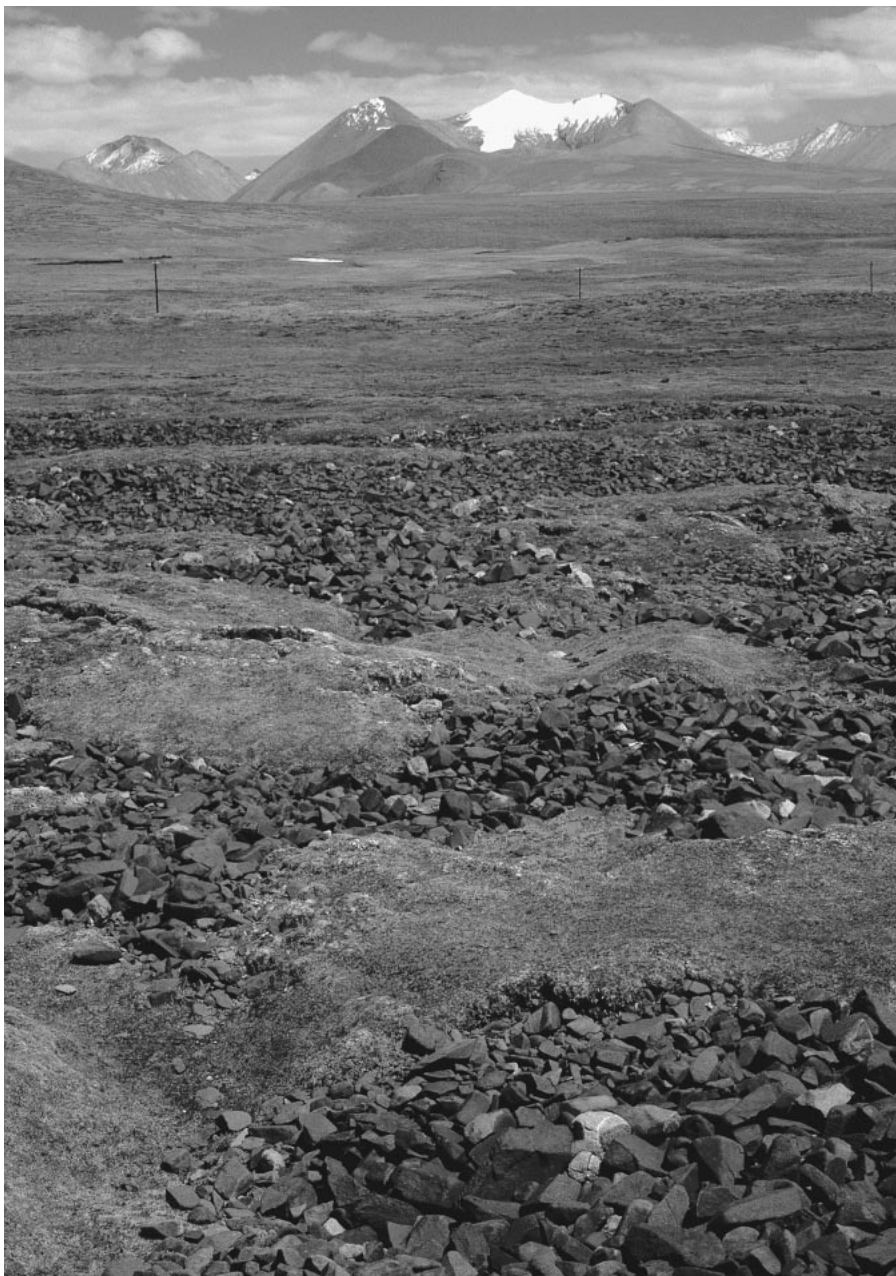


**FIGURE 6** Gyaco La (Gyaco Pass, 5220 m) on the Tibetan Plateau, showing the stone polygons that are a typical feature of a permafrost landscape. (Photo by Bruno Messerli)



especially the permafrost area, would be expected to decrease considerably in response to global climatic warming. Frozen ground has two environmental impacts. The first is a release of soil carbon to the atmosphere. Warming of frozen soils can thaw continuous permafrost, increase drainage, and hasten decomposition (Oechel et al 1994). The second is a northward movement of vegetation zones and permafrost in step with shifting isotherms (Melillo et al 1996). Simple climate/permafrost correlations applied to doubled CO<sub>2</sub> GCM simulations forecast permafrost well north of current distributions in the world (Anisimov and Nelson 1996). The movement (expansion and/or decline) of permafrost under changing climates, therefore, could be used as an indicator of changes in global climate and would help provide an understanding of how terrestrial ecosystems will respond to changes in the global climate.

The permafrost area on the Tibetan Plateau is about 1,500,000 km<sup>2</sup>, which is about 70% of the frozen land area in China (Zhang et al 1996). Permafrost plays a very important role in determining vegetation distribution and dynamics and in indicating changes and fluctuations in climate. Under present climatic conditions, observed data showed that the continuous permafrost occurred mainly in central and northwestern Tibet, ie, in about 30% of the total permafrost area. The alpine permafrost occurred in northeastern and southwestern peaks. The seasonal frozen ground was found in the north and east, and the instantaneous and isolated permafrost occurred in the south (Figure 2a). The permafrost pattern predicted by *AFI* is similar to observed data, apart from the alpine permafrost occupying part of the continuous permafrost areas in the central plateau and apart from isolated permafrost taking the place of the seasonal frozen ground in the eastern margin (Figure 2b). As with climatic gradient, there is permafrost in the northwest but not in the southeast. The permafrost pattern with climate gradient determines the vegetation distributions on the Tibetan Plateau. Namely, forests and some shrubland/meadow occur in the nonpermafrost areas; tem-

perate steppe, desert, and some shrubland/meadow occur on the seasonal frozen ground; and alpine steppe, desert, and ice/polar desert occur in the continuous permafrost areas.

Under climate warming conditions at the end of the next century, the boundary between continuous and discontinuous permafrost would shift toward the north of the Plateau by about 1–2° in latitude (Figure 2c). The continuous permafrost would largely disappear because increased temperatures would melt the underground ice, and about 70% of the total area on the Tibetan Plateau (Figure 2c) would be occupied by nonpermafrost area (instantaneous and isolated permafrost). The movement of permafrost would happen with the shift of vegetation zones to the north. Disappearance of permafrost and expansion of nonpermafrost would accelerate desertification in the plateau. This may be mainly because temperature increases would result in an increase in evaporation, although ice below ground would melt and precipitation would increase in most regions.

High mountains as vulnerable environments will also be impacted first and with the greatest intensity by anthropogenically induced climate change as a result of both physiological responses arising from the increased CO<sub>2</sub> available for photosynthesis and the responses of organisms to physical climatic changes (Haslett 1997). The equilibrium pattern of Tibetan biomes and the equilibrium responses of biomes to climate change and CO<sub>2</sub> enrichment were modeled using the improved BIOME3China model, but the dynamics of vegetation and carbon budget on the Plateau still need to be explicitly simulated. This is because there is a lack of information on the responses of phenology, growth, and reproduction in major vascular plant species to climate variations and environment manipulations in the Tibetan Plateau. The vertical changes in vegetation on the Tibetan Plateau are also very important. BIOME3China did not model these because of the lack of accurate climatic data in all high mountains and the shortcomings of BIOME3China itself in modeling vertical vegetation changes. This will clearly require further efforts.

#### AUTHOR

##### Jian Ni

Laboratory of Quantitative Vegetation Ecology, Institute of Botany, Chinese Academy of Sciences, Xiangshan Nanxincun 20, 100093 BEIJING, P. R. China, and Climate Impacts Group, Department of Ecology, Lund University, Sölvegatan 37, S-223 62 LUND, Sweden. nijian@public.east.cn.net

#### ACKNOWLEDGMENTS

This study was partly undertaken while the author was a guest scholar at the Department of Plant Ecology, Lund University, with funding from the Swedish Institute (SI). I am grateful to Martin Sykes and Colin Prentice for providing the BIOME3 model and a review. I also wish to thank Wolfgang Cramer for climate data and scenarios and Ming Dong for improving the English. The research for this study was jointly funded by the National Natural Science Foundation of China (NSFC 39700018, 39970154, 49731020) and the Chinese Academy of Sciences (KZ951-131-108).

## REFERENCES

- Anisimov OA, Nelson FE.** 1996. Permafrost distribution in the Northern Hemisphere under scenarios of climate change. *Global and Planetary Change* 14:59–72.
- Chinese Central Meteorological Office.** 1984. *Climatological Data of China*. Beijing: Meteorology Press of China.
- Editorial Committee for Vegetation of China.** 1980. *Vegetation of China*. Beijing: Science Press.
- Foley JA, Prentice IC, Ramankutty N, Levis S, Pollard D, Sitch S, Haxeltine A.** 1996. An integrated biosphere model of land surface processes, terrestrial carbon balance, and vegetation dynamics. *Global Biogeochemical Cycles* 10:603–628.
- Haslett JR.** 1997. Mountain ecology: organism responses to environmental change, an introduction. *Global Ecology and Biogeography Letters* 6:3–6.
- Haxeltine A, Prentice IC.** 1996. BIOME3: an equilibrium terrestrial biosphere model based on ecophysiological constraints, resource availability and competition among plant functional types. *Global Biogeochemical Cycles* 10:693–709.
- Hou XY, Sun SZ, Zhang JW, He MG, Wang YF, Kong DZ, Wang SQ.** 1982. *Vegetation Map of the People's Republic of China*. Beijing: Map Press of China.
- Hutchinson MF.** 1989. A new objective method for spatial interpolation of meteorological variables from irregular networks applied to the estimation of monthly mean solar radiation, temperature, precipitation and windrun. *Need for Climatic and Hydrologic Data in Agriculture in Southeast Asia*. Canberra: CSIRO.
- Intergovernmental Panel on Climate Change Working Group I (IPCC WGI).** 1996. *Climate Change 1995: The Science of Climate Change*. New York: Cambridge University Press.
- Johns TC, Carnell RE, Crossley JF, Gregory JM, Mitchell JFB, Senior CA, Tett SFB, Wood RA.** 1997. The second Hadley Centre coupled ocean-atmosphere GCM: model description, spinup and validation. *Climate Dynamics* 13:103–134.
- Liu XD, Zhang MF, Hui XY, Kang XC.** 1998. Contemporary climatic change of the Qinghai-Xizang Plateau and its response to greenhouse effect. *Scientia Geographica Sinica* 18:113–121.
- McGuire AD, Melillo JM, Kicklighter DW, Pan Y, Xiao X, Helfrich J, Moore B III, Vorosmarty CJ, Schloss AL.** 1997. Equilibrium responses of global net primary production and carbon storage to doubled atmospheric carbon dioxide: sensitivity to changes in vegetation nitrogen concentration. *Global Biogeochemical Cycles* 11:173–189.
- Melillo JM, McGuire AD, Kicklighter DW, Moore B III, Vorosmarty CJ, Schloss AL.** 1993. Global climate change and terrestrial net primary production. *Nature* 363:234–240.
- Melillo J, Prentice IC, Schulze E-D, Farquhar G, Sala O.** 1996. Terrestrial biotic responses to environmental change and feedbacks to climate. In: Houghton JT, Meira Filho LG, Callender BA, Harris N, Kattenberg A, Maskell K, editors. *Climate Change 1995: The Science of Climate Change*. Cambridge: Cambridge University Press, pp 445–482.
- Mitchell JFB, Johns TC, Gregory JM, Tett SFB.** 1995. Climate response to increasing levels of greenhouse gases and sulphate aerosols. *Nature* 376:501–504.
- Nelson FE, Outcalt SI.** 1987. A computational method for prediction and regionalization of permafrost. *Arctic and Alpine Research* 19:279–288.
- Ni J, Sykes MT, Prentice IC, Cramer W.** 1999. Modelling the vegetation of China using the process-based equilibrium terrestrial biosphere model BIOME3. *Global Ecology and Biogeography* (in press).
- Oechel WC, Cowles S, Grulke N, Hastings SJ, Lawrence B, Prudhomme T, Riechers G, Strain B, Tissue D, Vourlitis G.** 1994. Transient nature of CO<sub>2</sub> fertilization in Arctic tundra. *Nature* 371:500–503.
- Prentice IC, Cramer W, Harrison SP, Leemans R, Monserud RA, Solomon AM.** 1992. A global biome model based on plant physiology and dominance, soil properties and climate. *Journal of Biogeography* 19:117–134.
- Sykes MT, Prentice IC, Laarif F.** 1999. Quantifying the impact of global climate change on potential natural vegetation. *Climatic Change* 41:37–52.
- Xiao X, Melillo JM, Kicklighter DW, Pan Y, McGuire AD, Helfrich J.** 1998. Net primary production of terrestrial ecosystems in China and its equilibrium responses to changes in climate and atmospheric CO<sub>2</sub> concentration. *Acta Phytocologica Sinica* 22:97–118.
- Xiong Y, Li QK.** 1987. *Soil of China*. Beijing: Science Press.
- Zhang XS, Yang DA, Zhou GS, Liu CY, Zhang J.** 1996. Model expectation of impacts of global climate change on biomes of the Tibetan Plateau. In: Omasa K, Kai K, Taoda H, Uchijima Z, Yoshino M, editors. *Climate Change and Plants in East Asia*. Tokyo: Springer-Verlag, pp 25–38 + xxv–xxxix.
- Zhang XS.** 1983. The Tibetan Plateau in relation to the vegetation of China. *Annals of Missouri Botanical Garden* 70:564–570.
- Zheng D.** 1996. The system of physico-geographical regions of the Qinghai-Xizang (Tibet) Plateau. *Science in China (Series D)* 39:410–417.